Sensor-less Terrain Estimation and Torque Control of a Wheeled Mobile Robot

J.D.C.C RATHNAPALA, M.U.B JAYATHILAKE, R.M.U.K.H.M.K RATHNAYAKE, B.G.L.T SAMARANAYAKE, and Nalin HARISCHANDRA

(*Department of Electrical and Electronic Engineering, University of Peradeniya, Sri Lanka.*
chathushkachamith11@gmail.com, urithjayathilake@gmail.com,
harshanamadushanka110@gmail.com, lilantha@ee.pdn.ac.lk, nalin@ee.pdn.ac.lk)

Abstract: As unmanned electric wheeled mobile robots have been increasingly applied to high-speed operations in unknown environments, the wheel slip becomes a problem when the robot is either accelerating, decelerating, or turning at high speed. Ignoring the effect of wheel slip may cause the mobile robot to deviate from the desired path. In this paper a recently proposed method is implemented to estimate the surface conditions encountered by an unmanned wheeled mobile robot, without using extra sensors. The method is simple, economical and needs less processing power than for other methods. A reaction torque observer is used to obtain the rolling resistance torque and it is applied to a wheeled mobile robot to obtain the surface condition in real-time for each wheel. The slip information is observed by comparing the reaction torque of each wheel. The obtained slip information is then used to control the torque of both wheels using a torque controller. Wheel slip is minimized by controlling the torque of each wheel. Minimizing the slip improves the ability of the unmanned electric wheeled mobile robot to navigate in the desired path in an unknown environment, regardless of the nature of the surface.

Key words: Wheeled Mobile Robot; Reaction Torque Observer; Disturbance Observer; Terrain Estimation.

1 Introduction

Estimating the terrain for a Wheeled Mobile Robot (WMR) is a challenging task when slip information is absent. Wheeled mobile robots use different types of sensors to estimate the slip ratio and other surface conditions[2].

Ideally, the wheels of a WMR satisfy the condition of pure rolling without slipping in any direction[1]. Terrain estimation and torque control are essential to achieve maximum traction force[2]. In literature, several methods have been proposed to estimate the terrain and the nature of the surfaces using accelerometers, cameras, global positioning systems (GPS) and inertial measurement units (IMU)[1,10]. These methods are complex, expensive, need high processing power, and require more space.

In some WMR configurations, non-driving trailing wheels are introduced to find the slip ratio. However it is notsuitable when the slip ratio is small and if the WMR moves slowly. Similarly, in some other WMR configurations, driving front wheel is used where the rear wheels act as the trailing wheels[14]. The main drawback of this approach is that the trailing wheels also start to slip[7,15]. There are other approaches where disturbance torque observers are used with accelerometers to calculate the slip ratio[3,6]. Here the velocity is calculated by integrating the acceleration, where the errors in accelerometer also get integrated and accumulated. GPS sensor can also be used when calculating the velocity. But it is hard to calculate velocity using GPS when the robot is under the cover of trees or operates indoors, because wheeled mobile robots are supposed to be used both indoors and outdoors. In summary, using sensors to estimate terrain and the surface condition become problematic due to the limitations of the sensors.

This paper presents an implementation of a re-

cently proposed method to estimate the nature of the surface that the wheels of a WMR encounters, without using any additional sensors[1]. This information is then used to control the wheel torque of the WMR, so that it follows the desired path in spite of the different surface conditions encounter each wheel. Here, a reaction torque observer is used to obtain rolling resistance torque and it is used in the wheeled mobile robot control. The observer uses a model of the system along with the past measurements of both input and output trajectories of the system. The information taken by the observer is then used to navigate the WMR in different surface conditions by minimizing the slip and improving the ability of the WMR to follow the desired path without using any extra sensors[12].

2 Methodology

Terrain estimation is done without using extra sensors other than the current sensor and shaft encoders, which are usually used in any WMR[1]. Disturbance torque[3] experienced by each wheel is derived by implementing a reaction torque observer[6]. The reaction torque observer output is used to find the terrain condition and the wheel slip.

2.1 Motor Model

The motors used here were Permanent Magnet Direct current Motors (PMDM)[4]. The dynamic behavior of the motor can be described using differential equations, and accordingly Laplace transform and state space descriptions are obtained.

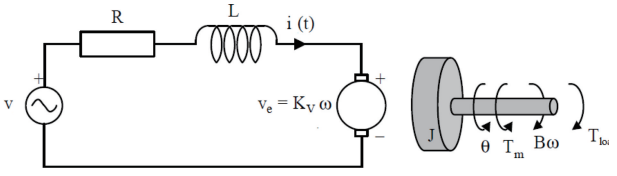

Fig. 1 PMDM diagram.

The mathematical model relates the input voltage tothe motor armature to the velocity of the motor. Two equations can be developed considering the electrical and mechanical characteristics of the motor[8]. The PMDM block diagram is shown in the Fig. 1.

V - Input voltage [V]

$i(t)$ - Armature current [A]

v_e - Back electromotive force [V]

$\omega(t)$ - Angular velocity of the rotor [rad/s]

T_{load} - Load torque [N.m]

J - Load inertia + Rotor inertia [kg.m^2]

B - Rotor viscous friction coefficient [Nm/(rad/s)]

K_v - Motor velocity constant or back emf Constant [V/(rad/s)]

R - Armature resistance [Ohm]

L - Armature inductance [H]

K_t - Motor torque constant [N.m/A]

T_m - Torque produced by motor [N.m]

Electrical characteristics give

$$V = i(t)\,R + L\frac{di(t)}{dt} + V_e \tag{1}$$

The back electromotive force (emf) can be modelled as,

$$V_e = K_v\omega(t) \tag{2}$$

The mechanical characteristics can be modelled as

$$T_m = T_{load} + J\frac{d\omega(t)}{dt} + B\omega(t) \tag{3}$$

where, the induced torque is modelled as,

$$T_m = K_t i(t) \tag{4}$$

2.2 State Space Model of the PMDM

Using the equations (1) and (2),

$$V = i(t)\,R + L\frac{di(t)}{dt} + K_v\omega(t) \tag{5}$$

$$\frac{di(t)}{dt} = \frac{V}{L} - \frac{R}{L}i(t) - \frac{K_v}{L}\omega(t) \tag{6}$$

Using the equations (3) and (4),

$$K_t i(t) = T_{load} + J\frac{d\omega(t)}{dt} + B\omega(t) \tag{7}$$

$$\frac{d\omega(t)}{dt} = -\frac{T_{load}}{J} + \frac{K_t}{J}i(t) - \frac{B}{J}\omega(t) \tag{8}$$

Defining the states as,

$$X = \begin{bmatrix} i(t) \\ \omega(t) \end{bmatrix}$$

State space model is obtained from (6) and (8) as,

$$\dot{X} = \begin{bmatrix} -\frac{R}{L} & -\frac{K_v}{L} \\ \frac{K_t}{J} & -\frac{B}{J} \end{bmatrix} X + \begin{bmatrix} \frac{1}{L} & 0 \\ 0 & -\frac{1}{J} \end{bmatrix} \begin{bmatrix} V \\ T_{load} \end{bmatrix}$$

$$Y = \begin{bmatrix} 1 & 0 \\ 0 & 1 \end{bmatrix} X$$

2.3 Block Diagram of the PMDM

Applying the Laplace transform to (5) and (7),

$$V(s) = I(s)\,R + LsI(s) + K_v\omega(s) \quad (9)$$

$$K_tI(s) = T_{load}(s) + Js\omega(s) + B\omega(s) \quad (10)$$

$$I(s) = \frac{-K_e\omega(s) + V(s)}{Ls + R} \quad (11)$$

$$\omega(s) = \frac{-K_tI(s) - T_{load}(s)}{Js + B} \quad (12)$$

The block diagram of the PMDM is shown in Fig. 2.

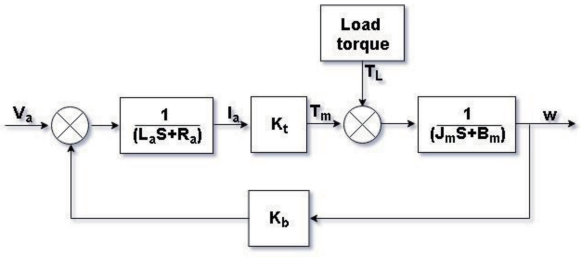

Fig. 2 Block Diagram of the PMDM model.

2.4 Experiment to Find Motor Constants

The motor parameters were found experimentally, and the details of the procedure can be found in [5]. Table 1 shows the PMDM parameters.

Table 1 Experimentally obtained PMDM parameters.

	Motor 1	Motor 2	Units
R_a	8.062	8.099	Ω
L_a	51.13	45.6	mH
$K_e = K_v$	0.1196	0.1192	V/(rad/s)
B	0.3711	0.5943	N m /(rad/s)
C	0.01901	0.01573	N m
J	$6.1016\text{x}10^{-4}$	$6.0825\text{x}10^{-4}$	kg * m^2

2.5 Observer Design

An observer is a system that provides an estimate of the internal states of the corresponding real system[9], by using the measurements of the inputs and outputs of the real system. It is typically implemented digitally in a microprocessor-based environment.

In an unknown terrain, the robot can encounter disturbance forces to the motion, which can result in deviation from the desired path. The observers have been designed to determine these disturbance forces, which appear as disturbance torques on the wheels[7].

In the present work it is assumed that the disturbances appear as load torques and viscous torques[10]. Any deviation from the desired path can be corrected if the disturbances are known. It takes the time-derivative of the speed, multiplies with the rotor inertia and deducts that product from the induced torque of the motor obtained by multiplying the motor curent by the torque constant of the motor. This difference is sent through a low pass filter with unity gain and a single pole at $s = -G$. The disturbance observer block diagram is shown in Fig. 3.

The low pass filter parameter (G) of the disturbance observer should be tuned to obtain the optimal performance of the system[1,3]. If it is too high, the system can become unstable and if it is too low, the system may not respond to high frequency disturbances sufficiently fast.

After that, rolling torqueis observed by further improving the above design to remove the viscous torque in the disturbance[11]. Rolling torque observer is used for the terrain estimation and torque control, and is designed by adding a slight modification, specifically, substracting the product of viscous friction coefficient and the motor speed from the induced torque term to the disturbance observer (see Fig. 4).

2.6 Torque Controller Design

When the robot moves ina uniform terrain, the reaction torque experienced by the two wheels should be the same. Hence to minimize the slip, the magnitude

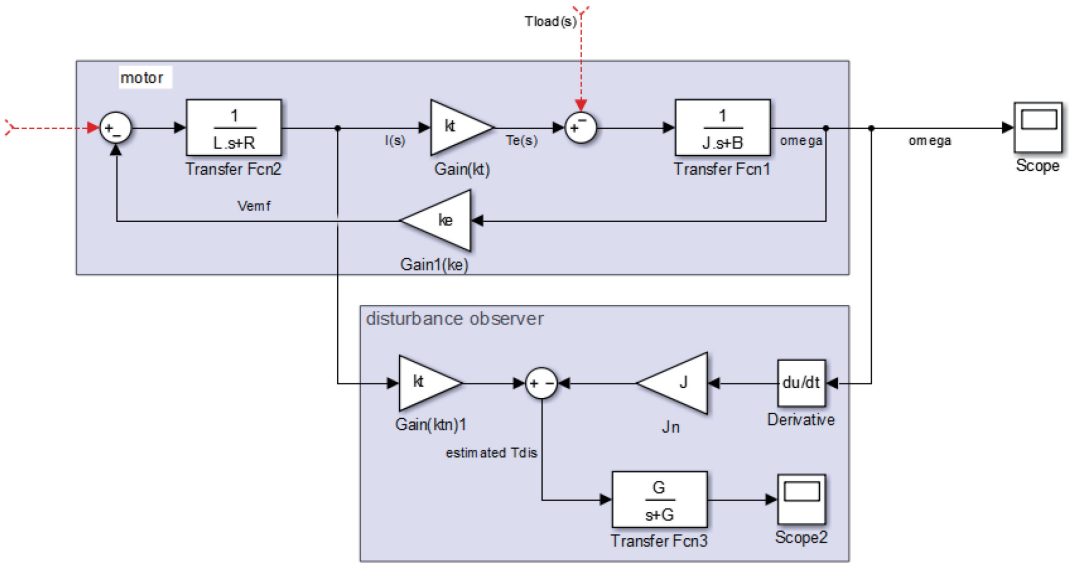

Fig. 3 Disturbance observer design.

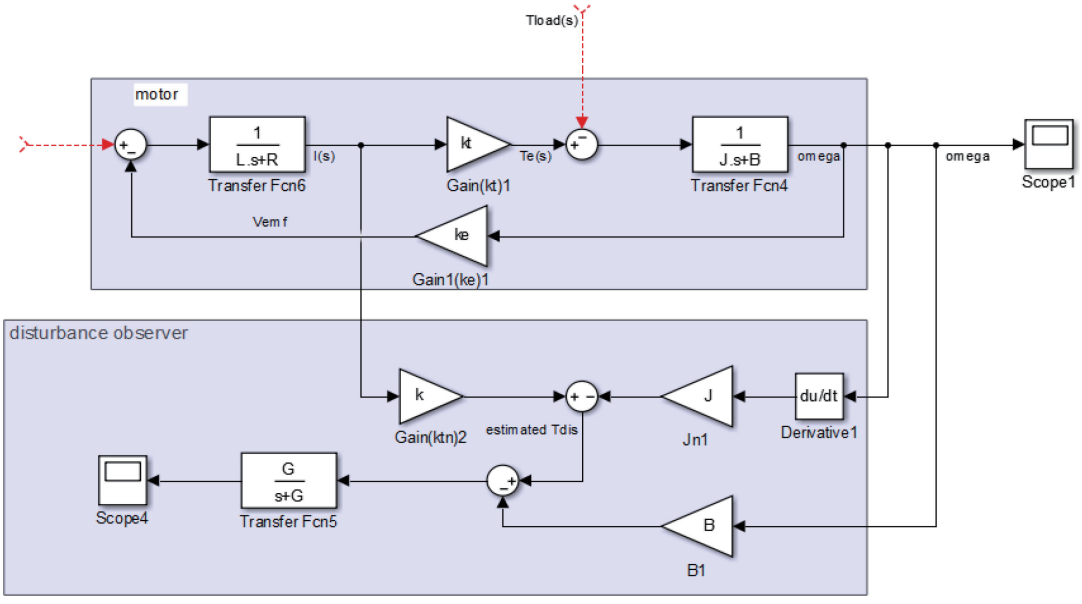

Fig. 4 Rolling torque observer design.

of the difference between the two reaction torques of the two wheels should be minimized.

The torque controller is designed to regulate the difference between the two reaction torques close to zero. Then the output is fed to the two reference speeds of the motors. This will slow down the motors until the slipping motor gets its grip back and the non-slipping motor will not cause its speed to change the pre-mapped path that the autonomous robot is following.

Due to practical reasons, a small region around the balance point of the two reaction torques was kept as a region of negligence. The torque controller will only activate if the difference between the two torques is greater than this region of negligence. If it is active, the absolute value of the torque difference is sent through a Proportional-Derivative (PD) controller, whose parameters are tuned to obtain the de-

sired closed loop torque profile. The torque controller is shown in Fig. 5.

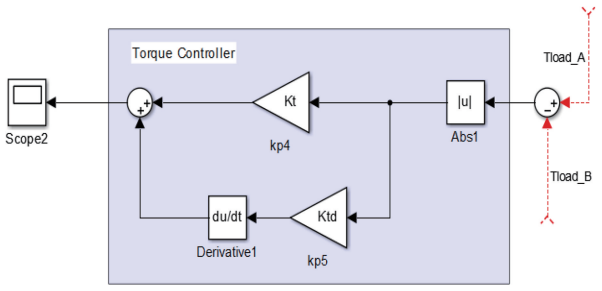

Fig. 5 Torque controller design.

2.7 Overall Controller Block Diagram

When a reaction torque is experienced by one motor, the difference of the reaction torques of the two motors is fed back to the reference speed of the opposite motor. The successful model was further improved by feeding a fraction of the controller output to the reference speed of the same motor. This controller model gave better results by following the desired path with a lower error. The complete schematic diagram of the overall controller is shown in Fig. 6.

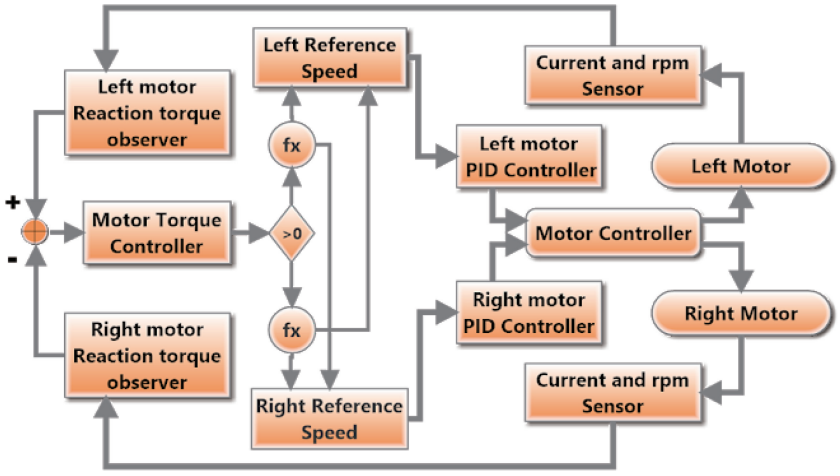

Fig. 6 Schematic diagram of the overall controller.

A high ratio of the reaction torque difference was given to the reference speed of the motor with less reaction torque, and vice versa.

3 Results

As the first step, the WMR was tested on a uniform floor by moving it in a linear path without using the terrain estimation and torque control algorithm. This procedure was followed to observe the variation of the reaction torques, reference speed and actual speed of each wheel for bench marking. Fig. 7 shows the experimental setup, which includes the WMR platform.

The real time plots of the reaction torques, reference speed and actual speed of each wheel are shown in Fig. 9. It is seen that the robot follows the reference speed while maintaining a very low variation of the reaction torque of each wheel. In this case, the reaction torques experienced by the wheels are almost the same.

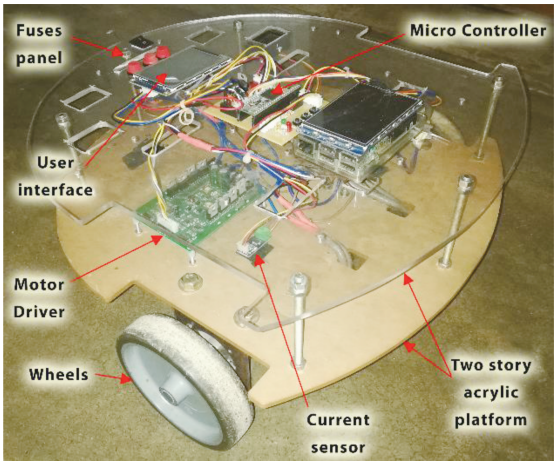

Fig. 7 WMR platform.

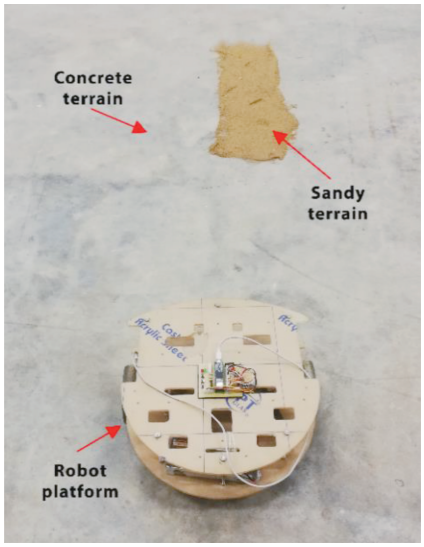

Fig. 8 Right wheel on a sandy terrain.

Next, the controller was tested in a specially created terrain conditions, where one wheel encounters a sandy terrain while the other is still on the uniform, smooth cement terrain, as shown in the Fig. 8. Without using the terrain estimator, the WMR deviates from the desired path. Our goal was to implement and test an algorithm that can minimize the error of deviation and follow the desired path. Here, as a proof-of-concept, the robot should follow a straight line in spite of the different terrain conditions that the two wheels experience.

When tested without using the controller, it can be observed that the robot tries to maintain its speed around the reference speed, as shown in Fig. 10.

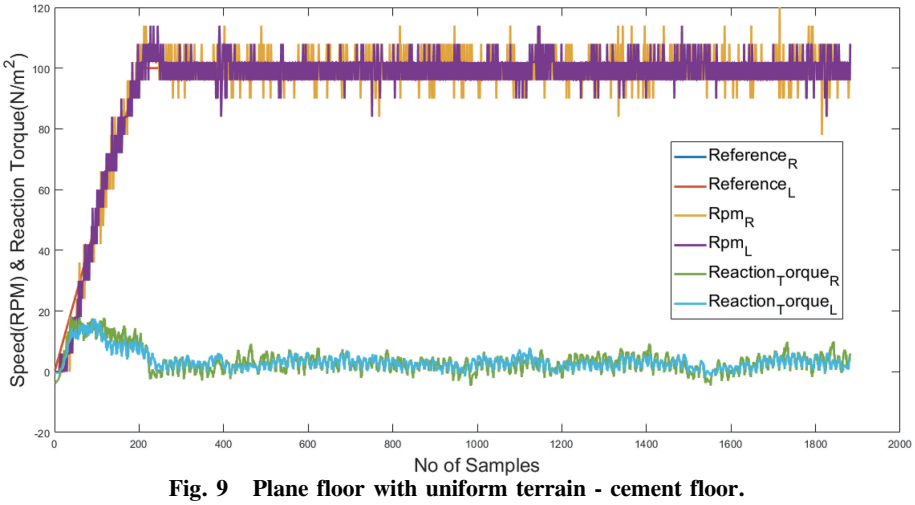

Fig. 9 Plane floor with uniform terrain - cement floor.

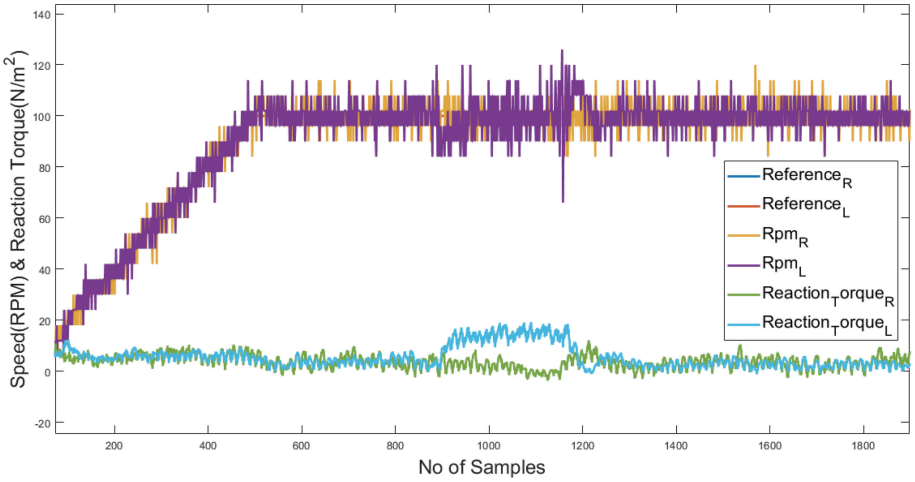

Fig. 10 Without algorithm - Left wheel on the sand surface.

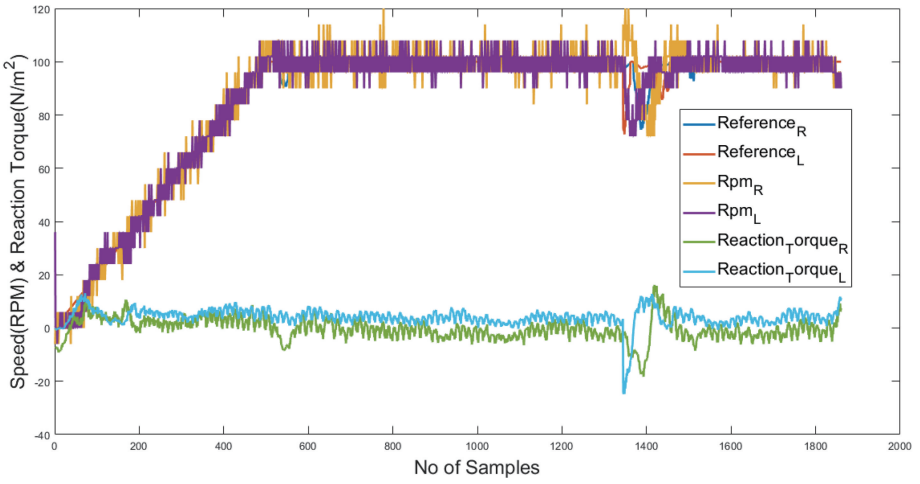

Fig. 11 With algorithm - Left wheel on the sand surface.

There is a clear difference between the reaction torques of the two wheels: one wheel on sand and the other wheel on cement floor.

When tested with the controller, the algorithm tries to keep the reaction torque difference around zero, as shown in Fig. 11. It is done by reducing the reference speed when there is a torque difference.

As shown in Fig. 12, the robot deviates from the desired path without the control algorithm. However, with the algorithm, the robot maintains the desired path with minimum error, as shown in Fig 13.

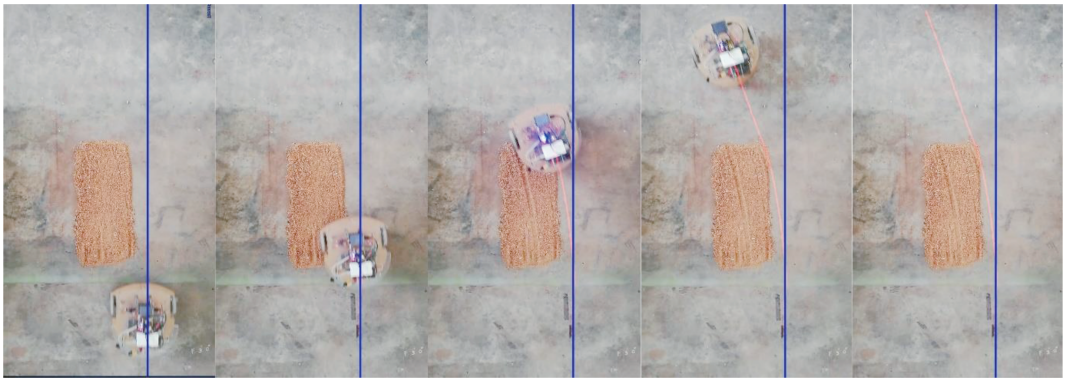

Fig. 12 Without algorithm - Left wheel on the sand surface.

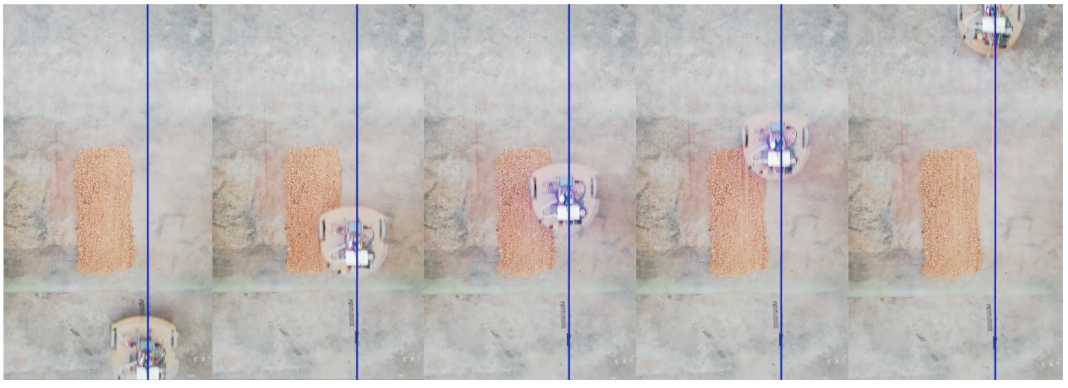

Fig. 13 With algorithm - Left wheel on the sand surface.

4 Conclusion

The objective of this work was to control a WMR, where each motor encountered different terrain conditions, without using any extra sensors. In the present work, a reaction torque observer was used to estimate the surface conditions. Moreover, noval algorithm was developed to control the torque of each motor such that the WMR followed a desired path in spite of the nature of the surface.

The simulation as well as the experimental results confirmed that the torque control implemented using reaction torque observer, where each wheel of the WMR encountered different terrain conditions, outperformed a similar system without this arrangement. In future work, the proposed torque control will be tested for WMR with more than two wheels.

References

[1] Arunya, S.D., Senadheera, P., Harsha, A.M., and Abeykoon, S. (2017) "Sensorless Terrain Estimation for a Wheeled Mobile Robot", 2017 *IEEE International Conference on Industrial and Information Systems* (ICIIS), 2017, [online] Available: https://ieeexplore.ieee.org/document/8300422

[2] Xu, Y. and Yung, K.L. (2005) "Forms of static friction, sliding friction and rolling friction" WTC2005-64050, World Tribology Congress III, September 12-16, 2005, Washington, D.C., USA.

[3] https://ocw.mit.edu (2010). *State Observers and State Feedback.* [online] Available: https://ocw.mit.edu/courses/electrical-engineering-and-computer-science/6-011-introduction-to-communication-control-and-signal-processing-spring-2010/readings/MIT6_011S10_chap06.pdf. [Accessed 05 Feb. 2018]

[4] Ismail, H. ALTAS (2007). *Dynamic Model of a Permanent Magnet DC Motor*. Karadeniz Technical University Faculty of Engineering Electrical and Electronics Engineering [online] Available:

[5] http://www.ihaltas.com/courses/fbe_elk5320/eng/projects/Project_37.pdf. [Accessed 05 Feb. 2018]

[6] Samer, S. Saab. and Raed Abi Kaed-Bey. (2001) *Parameter identification of a DC motor: An experimental approach.* 2001. The 8th IEEE International Conference on Electronics, Circuits and Systems, 2001. ICECS, Volume: 2. [Accessed 05 Feb. 2018].

[7] IslamS. M. Khalil and Asif Sabanovic. (2012) Action-*Reaction Based Parameters Identification and States Estimation of Flexible systems*. Turkish Journal of Electrical Engineering and Computer Sciences, 2012.

[8] Li, Zexiang and Canny, John. (1990). *Motion of Two Rigid Bodies with Rolling Constraint*. IEEE Transactions on Robotics and Automation, 1990.

[9] Pillay, Pragasan and Krishnan, R. (1988). *Modeling of Permanent Magnet Motor Drives*. IEEE Transactions on Industrial Electronics, 1988.

[10] Pillai, Branesh M. and Suthakorn, Jackrit. (2019) *Motion control applications: Observer based DC motor parameters estimation for novices*. International Journal of Power Electronics and Drive Systems, 2019.

[11] Sado, H., Sakai S. and Hori, Y. (1999). *Road condition estimation for traction control in electric vehicle*. Industrial Electronics, 1999. ISIE '99. Proceedings of the IEEE International Symposium on, Bled, 1999, pp. 973-978 vol.2.

[12] Yu Tian and Nilanjan Sarkar. (2014). *Control of a Mobile Robot Subject to Wheel Slip*. Published in Journal of Intelligent and Robotic Systems 2014.

[13] Debangshu Sadhukhan, Carl Moore, and Emmanuel Collins. (2004). *TERRAIN ESTIMATION USING INTERNAL SENSORS*. IASTED International Conference on Robotics and Applications, 2004.

[14] Abeykoon, A. M. H. S. and Ohnishi, K. (2005) *Traction force improvement of a two-wheel mobile manipulator by changing the center of gravity*. INDIN'05. 2005 3rd IEEE International Conference on Industrial Informatics, 2005, pp. 756-760.

[15] Karl Iagnemma and Steven Dubowsky. (2002) *Terrain estimation for high-speed rough-terrain autonomous vehicle navigation.* Proceedings of SPIE Conference on Unmanned Ground Vehicle Technology IV, pp. 256-266, 2002.

[16] Karl Iagnemma, Hassan Shibly, and Steven Dubowsky. (2002). *On-line Terrain Parameter Estimation for Planetary Rovers.* Proceedings of the 2002 IEEE International Conference on Robotics and Automation, Washington DC, vol. 3, pp. 3142-3147.